Journal of Applied Fluid Mechanics, Vol. 8, No. 2, pp. 243-254, 2015.
Available online at www.jafmonline.net, ISSN 1735-3572, EISSN 1735-3645.
DOI: 10.18869/acadpub.jafm.67.221.21518

On the Flow of Generalized Burgers' Fluid Induced by Sawtooth Pulses

Q. Sultan, M. Nazar †, U. Ali, and I. Ahmad

Centre for Advanced Studies in Pure and Applied Mathematics, Bahauddin Zakariya University, Multan, 60000, Pakistan

†*Corresponding Author Email: mudassar_666@yahoo.com*

(Received Sep 18, 2013; accepted May 19, 2014)

ABSTRACT

This paper presents a study for the MHD flow of an incompressible generalized Burgers' fluid through a rectangular duct in porous medium. The flow is generated due to the velocity sawtooth pulses applied on the duct. Exact solutions of the governing equations are obtained by using the Laplace transform and double finite Fourier sine transform in this order. The obtained solutions satisfy all the initial and boundary conditions and are written as a sum of steady and transient solutions. Graphs are plotted for both developing and retarding flows. The effects of magnetic parameter, porosity parameter, and various parameters of interest on the flow characteristics are discussed. The problem reduces to the flow between two plates in the absence of side walls.

Keywords: Generalized Burgers' fluid, Sawtooth pulses, MHD flow, Porous medium.

NOMENCLATURE

L	velocity gradient
μ	dynamic viscosity
V	velocity field
$\hat{k}$	unit vector along the z-directionchord
R	Darcy's resistance
k	permeability of the medium
ϕ	porosity
Ω	dimensionless magnetic parameter
ε	dimensionless porosity parameter
ρ	density
J	current density
T	time period
β	aspect ratio
B	total magnetic field
σ	electrical conductivity of the fluid
λ_1	relaxation time
λ_3	retardation time
λ_2	material parameter
λ_4	material parameter
β_0	strength of applied magnetic field
$H(\cdot)$	Heaviside unit step function
S	extra-stress tensor
A	first Rivlin-Ericksen tensor

1. INTRODUCTION

The study of fluid flows has numerous applications in medicine, industry and technology. In the last decade, non-Newtonian fluids have been studied extensively. Flow of such fluids through different geometries of cross-sections e.g., circular, triangular, rectangular, involve different types of solutions. Phenomena of flow through porous media occur in industry, geomechanics and biomechanics, e.g., filtration of fluids, flow of fluids through rocks and regulation of skin.

Hunt (1965) presented an analysis of laminar motion of a conducting liquid in a rectangular duct under a uniform transverse magnetic field. Johri and Singh (1998) discussed oscillating flow of a viscous liquid in a porous rectangular cross-section under the influence of periodic pressure gradient using finite cosine transforms. Tsangaris and Vlachakis (2003) solved Navier-Stokes equations to obtain the analytical solution of the fully developed laminar flow in a duct having a cross section of a right-angled isosceles triangle in the presence of oscillating pressure gradient. Fetecau and Corina Fetecau (2005) provided a set of solutions corresponding to two types of unsteady flows of an Oldroyd-B fluid in a channel of rectangular cross-section in the presence as well as in the absence of pressure gradient. Khan et al. (2007) analyzed the

influence of Hartman number on the flow of an Oldroyd-B fluid in a porous medium for the velocity, volume flux, and tangential stresses using the double Fourier sine transform. Ghosh and Sana (2008) constructed the hydromagnetic channel flow of Oldroyd-B fluid induced by tooth pulses. Fetecau et al. (2009) established the analytic solution for the velocity field and the shear stress, corresponding to the unsteady flow of an Oldroyd-B fluid in an infinite circular cylinder subject to a time-dependent couple by means of the Hankel transform. Mahmood et al. (2010) obtained exact solutions for the oscillatory motion of a generalized second grade fluid in an annular region between two cylinders. M. The study of Jarrahi et al. (2011) investigated the laminar developing flow through a curved pipe under steady, pure sinusoidal and pulsatile conditions. Seth et al. (2011) studied the unsteady hydromagnetic coquette flow of an incompressible electrically conducting fluid in a rotating system in the presence of a uniform transverse magnetic field through porous medium induced by the impulsive movement of the upper plate of the channel. Khan and Zeeshan (2011) investigated the unsteady magneto hydrodynamic flow of an Oldroyd-B fluid through a porous space induced by saw tooth pulses by using the Laplace transform method. Nazar et al. (2012) presented an analysis for the unsteady flow of an incompressible Maxwell fluid in an oscillating rectangular cross section for the velocity field and the associated shear stresses using the Fourier sine and Laplace transforms. Khan et al. (2012) extended the work of Nazar (2012) to Burgers' fluid. Sultan et al. (2013a), (2013b) obtained the analytic solutions for the unsteady MHD flow of Maxwell and Oldroyd-B fluids respectively, in long porous rectangular cross-section. Seth and Singh (2013) presented an analysis for the unsteady hydromagnetic couette flow of a viscous incompressible electrically conducting fluid in a rotating system with Hall effects in the presence of a uniform transverse magnetic field induced by the due to time dependent velocity oscillations of the upper plate in its own plane.

The objective of this paper is to study the unsteady flow of generalized Burgers' fluid through rectangular duct. The duct is brought into motion induced by the velocity sawtooth pulses applied on the duct in the presence of magnetic field. The problem is solved by introducing the non-dimensional variables. Laplace and Fourier sine transforms have been used as mathematical tools to solve the problem. The problem reduces to the flow between two plates, when the aspect ratio parameter (ratio of length to width) is zero. Solutions for Oldroyd-B, Maxwell, and Newtonian fluids are also obtained as limiting cases.

1. GOVERNING EQUATIONS

For the generalized Burgers' fluids, the Cauchy stress tensor is given by

$$\tau = -p\,I + S, \tag{1}$$

$$S + \lambda_1 \frac{\delta S}{\delta t} + \lambda_2 \frac{\delta^2 S}{\delta t^2} = \mu\left(A + \lambda_3 \frac{\delta A}{\delta t} + \lambda_4 \frac{\delta^2 A}{\delta t^2}\right), \tag{2}$$

where $-pI$ denotes the indeterminate spherical stress, $\lambda_3 < \lambda_1$ and λ_2 and λ_4 both having the dimension of square of time and

$$\frac{\delta^2 S}{\delta t^2} = \frac{\delta}{\delta t}\left(\frac{ds}{dt} - LS - SL^T\right). \tag{3}$$

We seek a velocity field V and stress field S of the form Nazar et al. (2012)

$$V = v(x, y, t) = w(x, y, t)\,\hat{k},\ S = S(x, y, t), \tag{4}$$

where $\hat{k}$ is the unit vector along the z-direction. If the fluid is at rest up to the moment $t = 0$, then

$$V(x, y, 0) = 0,\ S(x, y, 0) = \frac{\partial S(x, y, 0)}{\partial t} = 0. \tag{5}$$

Eqs. (1)- (3) and (5) give $S_{xx} = S_{xy} = S_{yy} = 0$ and the meaningful equations

$$\left(1 + \lambda_1 \frac{\partial}{\partial t} + \lambda_2 \frac{\partial^2}{\partial t^2}\right)\tau_1(x, y, t) = \mu\left(1 + \lambda_3 \frac{\partial}{\partial t} + \lambda_4 \frac{\partial^2}{\partial t^2}\right)\frac{\partial w(x, y, t)}{\partial x}, \tag{6}$$

$$\left(1 + \lambda_1 \frac{\partial}{\partial t} + \lambda_2 \frac{\partial^2}{\partial t^2}\right)\tau_2(x, y, t) = \mu\left(1 + \lambda_3 \frac{\partial}{\partial t} + \lambda_4 \frac{\partial^2}{\partial t^2}\right)\frac{\partial w(x, y, t)}{\partial y}, \tag{7}$$

Where $\tau_1 = S_{xz}(x, y, t)$ and $\tau_2 = S_{yz}(x, y, t)$ are the non-zero shear stresses.

The Darcy's resistance R for a generalized Burgers' fluid satisfies the following expression

$$\left(1 + \lambda_1 \frac{\partial}{\partial t} + \lambda_2 \frac{\partial^2}{\partial t^2}\right)R = -\frac{\mu\phi}{k}\left(1 + \lambda_3 \frac{\partial}{\partial t} + \lambda_4 \frac{\partial^2}{\partial t^2}\right)V, \tag{8}$$

A uniform Magnetic field $J \times B$ is applied to the fluid. It is assumed that the external electric field and the induced magnetic field are negligible such that the magnetic Reynolds number is small. Further it is assumed that the magnetic field is perpendicular to the velocity field.
Thus the Lorentz force due to magnetic field becomes

$$J \times B = -\sigma\,\beta_0^2 V, \tag{9}$$

The balance of linear momentum which governs the MHD flow through porous medium becomes

$$\rho \frac{dV}{dt} = \nabla \cdot \tau + J \times B + R, \tag{10}$$

We consider the unsteady flow of an incompressible, electrically conducting generalized Burgers' fluid through a duct of rectangular cross section whose sides are at $x = 0, x = d, y = 0$ and $y = h$. Initially, the duct and the fluid are at rest. At time $t = 0^+$ the duct starts moving induced by velocity sawtooth pulses applied on

the duct.
In view of Eqs. (4) and (6)-(10), the governing equation leads to

$$\rho\left(1+\lambda_1\frac{\partial}{\partial t}+\lambda_2\frac{\partial^2}{\partial t^2}\right)\frac{\partial w(x,y,t)}{\partial t}=$$
$$\mu\left(1+\lambda_3\frac{\partial}{\partial t}+\lambda_4\frac{\partial^2}{\partial t^2}\right)\left(\frac{\partial^2}{\partial x^2}+\frac{\partial^2}{\partial y^2}\right)w(x,y,t)$$
$$-\sigma\beta_0^2\left(1+\lambda_1\frac{\partial}{\partial t}+\lambda_2\frac{\partial^2}{\partial t^2}\right)w(x,y,t)$$
$$-\frac{\mu\phi}{k}\left(1+\lambda_3\frac{\partial}{\partial t}+\lambda_4\frac{\partial^2}{\partial t^2}\right)w(x,y,t). \quad (11)$$

We consider the following initial and boundary conditions

$$w(x,y,0)=\frac{\partial w(x,y,0)}{\partial t}=\frac{\partial^2 w(x,y,0)}{\partial t^2}=0,$$
$$x\in(0,d),\ y\in(0,h), \quad (12)$$

$$w(0,y,t)=w(d,y,t)=w(x,0,t)=w(x,h,t)=U f(t), \quad (13)$$

for all t, where $f(t)$ denotes the sawtooth pulses which is an even periodic function.
Introducing the following non-dimensional relations

$$w^*=\frac{w}{U},\ x^*=\frac{x}{d},\ y^*=\frac{y}{h},\ z^*=\frac{z}{d}, \quad (14a)$$

$$t^*=\frac{t\upsilon}{d^2},\ \lambda_1^*=\frac{\lambda_1\upsilon}{d^2},\ \lambda_2^*=\frac{\lambda_2\upsilon^2}{d^4},\ \lambda_3^*=\frac{\lambda_3\upsilon}{d^2}, \quad (14b)$$

$$\lambda_4^*=\frac{\lambda_4\upsilon^2}{d^4},\ \tau_1=\frac{dS_{xz}}{\mu U},\ \tau_2=\frac{dS_{yz}}{\mu U}. \quad (14c)$$

Eqs. (6), (7) and (11)-(13) in dimensionless form become

$$\left(1+\lambda_1\frac{\partial}{\partial t}+\lambda_2\frac{\partial^2}{\partial t^2}\right)\tau_1(x,y,t)=$$
$$\left(1+\lambda_3\frac{\partial}{\partial t}+\lambda_4\frac{\partial^2}{\partial t^2}\right)\frac{\partial w(x,y,t)}{\partial x}, \quad (15)$$

$$\left(1+\lambda_1\frac{\partial}{\partial t}+\lambda_2\frac{\partial^2}{\partial t^2}\right)\tau_2(x,y,t)=$$
$$\left(1+\lambda_3\frac{\partial}{\partial t}+\lambda_4\frac{\partial^2}{\partial t^2}\right)\frac{\partial w(x,y,t)}{\partial y}, \quad (16)$$

$$\left(1+\lambda_1\frac{\partial}{\partial t}+\lambda_2\frac{\partial^2}{\partial t^2}\right)\frac{\partial w(x,y,t)}{\partial t}=$$
$$\left(1+\lambda_3\frac{\partial}{\partial t}+\lambda_4\frac{\partial^2}{\partial t^2}\right)\left(\frac{\partial^2}{\partial x^2}+\beta^2\frac{\partial^2}{\partial y^2}\right)w(x,y,t)$$
$$-\Omega\left(1+\lambda_1\frac{\partial}{\partial t}+\lambda_2\frac{\partial^2}{\partial t^2}\right)w(x,y,t)$$
$$-\varepsilon\left(1+\lambda_3\frac{\partial}{\partial t}+\lambda_4\frac{\partial^2}{\partial t^2}\right)w(x,y,t). \quad (17)$$

while the initial and boundary conditions become

$$w(x,y,0)=\frac{\partial w(x,y,0)}{\partial t}=\frac{\partial^2 w(x,y,0)}{\partial t^2}=0,$$
$$for\ x\in[0,1],\ y\in[0,1], \quad (18)$$

$$w(0,y,t)=w(1,y,t)=w(x,0,t)=w(x,1,t)=f(t), \quad (19)$$

where $\beta=\frac{d}{h},\Omega=\frac{\sigma\beta_0^2 d^2}{\upsilon\rho},\varepsilon=\frac{\phi d^2}{k}$ and the asterisks have been omitted for simplicity.

According to the nature of $f(t)$, the boundary conditions in mathematical form may be expressed as [8]

$$w(0,y,t)=w(1,y,t)=w(x,0,t)=w(x,1,t)=$$
$$\frac{1}{T}\left(tH(t)+\frac{1}{2}\sum_{p=1}^{\infty}(-1)^p(t-pT)H_{pT}(t)\right), \quad (20)$$

Where $H(\cdot)$ is defined as $H_{pT}(t)=0$ for $t\le pT$ and $H_{pT}(t)=1$ for $t>pT$.

2. CALCULATION OF VELOCITY FILED

Applying Laplace transform to Eq. (17), using initial conditions given in Eq. (18), we obtain the following problem

$$\left(1+\lambda_1 q+\lambda_2 q^2\right)q\bar{w}(x,y,q)=$$
$$\left(1+\lambda_3 q+\lambda_4 q^2\right)\left(\frac{\partial^2}{\partial x^2}+\beta^2\frac{\partial^2}{\partial y^2}\right)\bar{w}(x,y,q)$$
$$-\Omega\left(1+\lambda_1 q+\lambda_2 q^2\right)\bar{w}(x,y,q)$$
$$-\varepsilon\left(1+\lambda_3 q+\lambda_4 q^2\right)\bar{w}(x,y,q). \quad (21)$$

and the Laplace transform $\bar{w}(x,y,q)$ of the function $w(x,y,t)$ has to satisfy the boundary conditions

$$\bar{w}(0,y,q)=\bar{w}(1,y,q)=\bar{w}(x,0,q)=\bar{w}(x,1,q)=$$
$$\frac{1}{T}\left(\frac{1}{q^2}+\frac{1}{2}\sum_{p=1}^{\infty}(-1)^p exp(-pTq)\frac{1}{q^2}\right), \quad (22)$$

Here we have used the property

$$L\left(H_a(t)g(t-a)\right)=exp[-as]\,G(s).$$

Multiplying both sides of Eq. (20) by $sin(\xi_m x)\ sin(\lambda_n y)$, where $\xi_m=m\pi$ and $\lambda_n=n\pi$, integrating then with respect to x from 0 to 1, with respect to y from 0 to 1, employing the methodology of [8] and taking into account the corresponding conditions given in Eq. (22), we obtain

$$\bar{w}_s(m,n,q)=\frac{a_{mn}\lambda_{mn}^2}{Tq^2}\left[\frac{1}{q^2}-\left[\{1+\lambda_3 q+\lambda_4 q^2\}/\right.\right.$$
$$\{\lambda_2 q^3+(\lambda_1+\lambda_2\Omega+\lambda_4(\lambda_{mn}^2+\varepsilon))q^2$$
$$\left.\left.+(1+\lambda_1\Omega+\lambda_3(\lambda_{mn}^2+\varepsilon))q+\Omega+\lambda_{mn}^2+\varepsilon)\}\right]\right]$$
$$\times(1+2\sum_{p=1}^{\infty}(-1)^p exp(-pTq)), \quad (23)$$

Where

$$a_{mn}=\frac{[1-(-1)^m][1-(-1)^n]}{\xi_m\lambda_n}, \tag{24}$$

$$\lambda_{mn}{}^2=\xi_m{}^2+\beta^2\lambda_n{}^2,\ m,n=1,2,3...\ . \tag{25}$$

Writing Eq. (23) in the following equivalent form

$$\bar{w}_s(m,n,q)=\frac{a_{mn}}{T}[\frac{1}{q^2}-[\{\lambda_2q^3+(\lambda_1+\lambda_2\Omega+\lambda_4+\varepsilon)q^2+(1+\lambda_1\Omega+\lambda_3\varepsilon)q+\Omega+\varepsilon)\}/\{\lambda_2q^3+(\lambda_1+\lambda_2\Omega+\lambda_4(\lambda_{mn}{}^2+\varepsilon))q^2+(1+\lambda_1\Omega+\lambda_3(\lambda_{mn}{}^2+\varepsilon))q+\Omega+\lambda_{mn}{}^2+\varepsilon)\}]\times(1+2\sum_{p=1}^{\infty}(-1)^p exp(-pTq)). \tag{26}$$

Let us take

$$\bar{B}_s(m,n,q)=[\lambda_2q^3+(\lambda_1+\lambda_2\Omega+\lambda_4\varepsilon)q^2+(1+\lambda_1\Omega+\lambda_3\varepsilon)q+\Omega+\varepsilon)]/[\lambda_2q^3+(\lambda_1+\lambda_2\Omega+\lambda_4(\lambda_{mn}{}^2+\varepsilon))q^2+(1+\lambda_1\Omega+\lambda_3(\lambda_{mn}{}^2+\varepsilon))q+\Omega+\lambda_{mn}{}^2+\varepsilon)]\ . \tag{27}$$

Eq. (27) can also be written as [8]

$$\bar{B}_s(m,n,q)=(q^3+aq^2+bq+c)/[q^2(q-q_{1,mn})(q-q_{2,mn})(q-q_{3,mn})] \tag{28}$$

where

$$a=\frac{\lambda_1+\lambda_2\Omega+\lambda_4\varepsilon}{\lambda_2},b=\frac{1+\lambda_1\Omega+\lambda_3\varepsilon}{\lambda_2},c=\frac{\Omega+\varepsilon}{\lambda_2},$$

$$q_{i,mn}=s_{i,mn}-\frac{\lambda_1+\lambda_2\Omega+\lambda_4(\lambda_{mn}{}^2+\varepsilon)}{3\lambda_2}$$

for $i=1,2,3.$ (29)

In the above relations

$$s_{1,mn}=\left(-\frac{\beta_{1,mn}}{2}+\sqrt{\frac{\beta_{1,mn}{}^2}{4}+\frac{\alpha_{1,mn}{}^3}{27}}\right)^{1/3}+\left(-\frac{\beta_{1,mn}}{2}-\sqrt{\frac{\beta_{1,mn}{}^2}{4}+\frac{\alpha_{1,mn}{}^3}{27}}\right)^{1/3}, \tag{30}$$

$$s_{2,mn}=Z\left(-\frac{\beta_{1,mn}}{2}+\sqrt{\frac{\beta_{1,mn}{}^2}{4}+\frac{\alpha_{1,mn}{}^3}{27}}\right)^{1/3}+Z^2\left(-\frac{\beta_{1,mn}}{2}-\sqrt{\frac{\beta_{1,mn}{}^2}{4}+\frac{\alpha_{1,mn}{}^3}{27}}\right)^{1/3}, \tag{31}$$

$$s_{3,mn}=Z^2\left(-\frac{\beta_{1,mn}}{2}+\sqrt{\frac{\beta_{1,mn}{}^2}{4}+\frac{\alpha_{1,mn}{}^3}{27}}\right)^{1/3}+Z\left(-\frac{\beta_{1,mn}}{2}-\sqrt{\frac{\beta_{1,mn}{}^2}{4}+\frac{\alpha_{1,mn}{}^3}{27}}\right)^{1/3}. \tag{32}$$

Where

$$\alpha_{1,mn}=\frac{1+\lambda_1\Omega+\lambda_3(\lambda_{mn}{}^2+\varepsilon)}{\lambda_2}-\frac{(\lambda_1+\lambda_2\Omega+\lambda_4(\lambda_{mn}{}^2+\varepsilon))^2}{3\lambda_2{}^2}, \tag{33}$$

$$\beta_{1,mn}=\frac{\lambda_{mn}{}^2+\Omega+\varepsilon}{\lambda_2}+2\frac{(1+\lambda_1\Omega+\lambda_3(\lambda_{mn}{}^2+\varepsilon))^3}{27\lambda_2{}^3}-\frac{(\lambda+\lambda_2\Omega+\lambda_4(\lambda_{mn}{}^2+\varepsilon))(1+\lambda_1\Omega+\lambda_3(\lambda_{mn}{}^2+\varepsilon))}{3\lambda_2{}^2}, \tag{34}$$

$$Z=\frac{-1+i\sqrt{3}}{2}. \tag{35}$$

we get $Re(q_i)<0$ if $\lambda_1\lambda_3-\lambda_2+\lambda_4>2\sqrt{\lambda_1\lambda_2\lambda_4}$ provided $\lambda_1,\lambda_2,\lambda_3,\lambda_4>0$.

An equivalent suitable representation of the Eq. (28) is

$$\bar{B}_s(m,n,q)=-\frac{1}{q_{1,mn}q_{2,mn}q_{3,mn}}[b+c(\frac{1}{q_{1,mn}}+\frac{1}{q_{2,mn}}+\frac{1}{q_{3,mn}}+\frac{1}{q})]\frac{1}{q}+\frac{\varphi_{1,mn}}{(q_{1,mn}-q_{2,mn})(q_{1,mn}-q_{3,mn})}\frac{1}{(q-q_{1,mn})}+\frac{\varphi_{2,mn}}{(q_{2,mn}-q_{1,mn})(q_{2,mn}-q_{3,mn})}\frac{1}{(q-q_{2,mn})}+\frac{\varphi_{3,mn}}{(q_{3,mn}-q_{1,mn})(q_{3,mn}-q_{2,mn})}\frac{1}{(q-q_{3,mn})}, \tag{36}$$

Where

$$\varphi_{j,mn}=\frac{q_{j,mn}{}^3+aq_{j,mn}{}^2+bq_{j,mn}+c}{q_{j,mn}{}^2},\ j=1,2,3. \tag{37}$$

Inverting Eq. (36) by means of Laplace transform, we obtain

$$B(m,n,t)=-\frac{1}{q_{1,mn}q_{2,mn}q_{3,mn}}[b+c(\frac{1}{q_{1,mn}}+\frac{1}{q_{2,mn}}+\frac{1}{q_{3,mn}}+t)]+\frac{\varphi_{1,mn}\exp(q_{1,mn}t)}{(q_{1,mn}-q_{2,mn})(q_{1,mn}-q_{3,mn})}+\frac{\varphi_{2,mn}\exp(q_{2,mn}t)}{(q_{2,mn}-q_{1,mn})(q_{2,mn}-q_{3,mn})}+\frac{\varphi_{3,mn}\exp(q_{3,mn}t)}{(q_{3,mn}-q_{1,mn})(q_{3,mn}-q_{2,mn})}. \tag{38}$$

Inversion of Eq. (26) by means of the Fourier sine and Laplace transforms and using Eq. (38), results in

$$w(m,n,t)=\frac{1}{T}\left(tH(t)+\frac{1}{2}\sum_{p=1}^{\infty}(-1)^p(t-pT)H_{pT}(t)\right)-\frac{16}{T}\sum_{m,n=0}^{\infty}\frac{\sin(\xi_Mx)}{\xi_M}\frac{\sin(\lambda_Ny)}{\lambda_N}[-\frac{1}{q_{1,MN}q_{2,MN}q_{3,MN}}\{b+c(\frac{1}{q_{1,MN}}+\frac{1}{q_{2,MN}}+\frac{1}{q_{3,MN}}+t)\}+\frac{\varphi_{1,MN}\exp(q_{1,MN}t)}{(q_{1,MN}-q_{2,MN})(q_{1,MN}-q_{3,MN})}+\frac{\varphi_{2,MN}\exp(q_{2,MN}t)}{(q_{2,MN}-q_{1,MN})(q_{2,MN}-q_{3,MN})}+\frac{\varphi_{3,MN}\exp(q_{3,MN}t)}{(q_{3,MN}-q_{1,MN})(q_{3,MN}-q_{2,MN})}]H(t)$$

$$-2\sum_{p=1}^{\infty}(-1)^p\frac{16}{T}\sum_{m,n=0}^{\infty}\frac{\sin(\xi_Mx)}{\xi_M}\frac{\sin(\lambda_Ny)}{\lambda_N}$$

$$[-\frac{1}{q_{1,MN}q_{2,MN}q_{3,MN}}[b+c(\frac{1}{q_{1,MN}}+\frac{1}{q_{2,MN}}+\frac{1}{q_{3,MN}}$$
$$+t-pT)]+\frac{\varphi_{1,MN}\exp(q_{1,MN}(t-pT))}{(q_{1,MN}-q_{2,MN})(q_{1,MN}-q_{3,MN})}$$
$$+\frac{\varphi_{2,MN}\exp(q_{2,MN}(t-pT))}{(q_{2,MN}-q_{1,MN})(q_{2,MN}-q_{3,MN})}$$
$$+\frac{\varphi_{3,MN}\exp(q_{3,MN}(t-pT))}{(q_{3,MN}-q_{1,MN})(q_{3,MN}-q_{2,MN})}]H_{pT}(t), \quad (39)$$

Where $M=2m-1$ and $N=2n-1$.

3. CALCULATION OF TANGENTIAL STRESS

Applying Laplace transform to Eqs. (15) and (16), we have the expressions

$$\bar{\tau}_1(x,y,q)=\frac{(1+\lambda_3 q+\lambda_4 q^2)}{(1+\lambda_1 q+\lambda_2 q^2)}\frac{\partial\bar{w}(x,y,q)}{\partial x}, \quad (40)$$

$$\bar{\tau}_2(x,y,q)=\frac{(1+\lambda_3 q+\lambda_4 q^2)}{(1+\lambda_1 q+\lambda_2 q^2)}\frac{\partial\bar{w}(x,y,q)}{\partial y}, \quad (41)$$

Using Eq. (26) in the above expressions, we have

$$\bar{\tau}_1(x,y,q)=-\frac{16}{T}\sum_{m,n=0}^{\infty}\cos(\xi_M x)\frac{\sin(\lambda_N y)}{\lambda_N}$$
$$\frac{(1+\lambda_3 q+\lambda_4 q^2)}{(1+\lambda_1 q+\lambda_2 q^2)}(q^3+aq^2+bq+c)/$$
$$[q^2(q-q_{1,mn})(q-q_{2,mn})(q-q_{3,mn})]$$
$$\left(1+\frac{1}{2}\sum_{p=1}^{\infty}\exp(-pTq)\right), \quad (42)$$

$$\bar{\tau}_2(x,y,q)=-\frac{16}{T}\sum_{m,n=0}^{\infty}\cos(\lambda_N y)\frac{\sin(\xi_M x)}{\xi_M}$$
$$\frac{(1+\lambda_3 q+\lambda_4 q^2)}{(1+\lambda_1 q+\lambda_2 q^2)}(q^3+aq^2+bq+c)/$$
$$[q^2(q-q_{1,mn})(q-q_{2,mn})(q-q_{3,mn})]$$
$$\left(1+\frac{1}{2}\sum_{p=1}^{\infty}\exp(-pTq)\right). \quad (43)$$

Let us take

$$\bar{A}(q)=\frac{(1+\lambda_3 q+\lambda_4 q^2)}{(1+\lambda_1 q+\lambda_2 q^2)}, \quad (44)$$

which can also be written in the form

$$\bar{A}(q)=a_2+a_3\frac{q+a_1}{(q+a_1)^2-b_1^2}$$
$$+a_4\frac{b_1}{(q+a_1)^2-b_1^2}, \quad (45)$$

Where

$$b_1=\frac{\sqrt{\lambda_1^2-4\lambda_2}}{2\lambda_2},\ a_2=\frac{\lambda_4}{\lambda_2},\ a_3=\frac{\lambda_2\lambda_3-\lambda_1\lambda_4}{\lambda_2^2}$$
$$a_1=\frac{\lambda_1}{2\lambda_2}, a_4=\frac{2\lambda_2(\lambda_2-\lambda_4)-\lambda_1(\lambda_2\lambda_3-\lambda_1\lambda_4)}{\lambda_2^2\sqrt{\lambda_1^2-4\lambda_2}}, \quad (46)$$

Where $\lambda_1^2-4\lambda_2>0$.

Applying the inverse Laplace transform to Eq. (45), we obtain

$$A(t)=a_2+a_3\cosh(b_1 t)\exp(-a_1 t)$$
$$+a_4\sinh(b_1 t)\exp(-a_1 t). \quad (47)$$

Let

$$\tau(M,N,t)=(A*B)(t)$$
$$=\int_0^t A(t-q)B(M,N,q)\,dq, \quad (48)$$

Using Eqs. (38) and (47) in the above equation, we obtain

$$\tau(M,N,t)=\int_0^t[a_2+a_3\cosh(b_1(t-q))\exp(-a_1(t-q))$$
$$+a_4\sinh(b_1(t-q))\exp(-a_1(t-q))][-\frac{1}{q_{1,MN}q_{2,MN}q_{3,MN}}$$
$$\{b+c(\frac{1}{q_{1,MN}}+\frac{1}{q_{2,MN}}+\frac{1}{q_{3,MN}}+q-pT)\}$$
$$+\frac{\varphi_{1,MN}\exp(q_{1,MN}q)}{(q_{1,MN}-q_{2,MN})(q_{1,MN}-q_{3,MN})}$$
$$+\frac{\varphi_{2,MN}\exp(q_{2,MN}q)}{(q_{2,MN}-q_{1,MN})(q_{2,MN}-q_{3,MN})}$$
$$+\frac{\varphi_{3,MN}\exp(q_{3,MN}q)}{(q_{3,MN}-q_{1,MN})(q_{3,MN}-q_{2,MN})}]dq. \quad (49)$$

Finally, inversion of Eqs. (42) and (43) by Laplace transform and using Eq. (49), give

$$\tau_1(x,y,t)=-\frac{16}{T}\sum_{m,n=0}^{\infty}\cos(\xi_M x)\frac{\sin(\lambda_N y)}{\lambda_N}$$
$$[\tau(M,N,t)H(t)+2\sum_{p=1}^{\infty}(-1)^p\tau(M,N,t-pT)H_{pT}(t)], \quad (50)$$

$$\tau_2(x,y,t)=-\frac{16}{T}\sum_{m,n=0}^{\infty}\cos(\lambda_N y)\frac{\sin(\xi_M x)}{\xi_M}$$
$$[\tau(M,N,t)H(t)+2\sum_{p=1}^{\infty}(-1)^p\tau(M,N,t-pT)H_{pT}(t)]. \quad (51)$$

4. RESULTS AND DISCUSSIONS

In the above work, exact solutions for velocity field and associated tangential stresses for MHD flow of generalized Burgers' fluid through rectangular cross-section have been established. The motion is generated by the velocity sawtooth pulses applied on the duct. Laplace and double Fourier sine transforms have been used in this order as mathematical tools to solve the present problem. The effects of pertinent parameters are seen on the velocity profile by plotting several graphs.

The influence of material constants λ_1, λ_2, λ_3 and λ_4 on velocity profile verses y is shown in Figs. (1)-(4). According to the nature of pulses applied on the duct, developing flow corresponds to $t=0.5$ and the

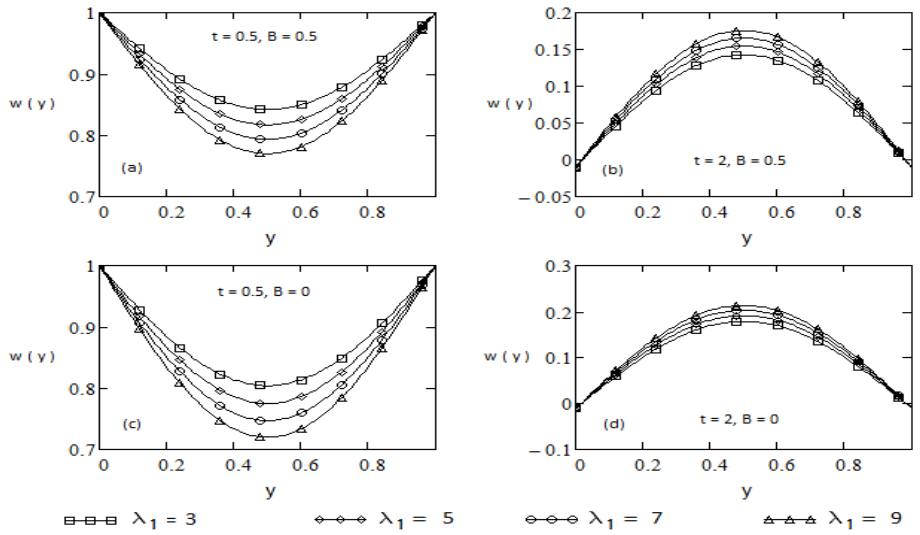

Fig. 1. Velocity profiles for duct motion induced by sawtooth pulses for Generalized Burgers' fluid for different values of λ_1. Other parameters and values are taken as $x = 0.5,\ \lambda_2 = 4,\ \lambda_3 = 2, \lambda_4 = 8,\ T = 1, \Omega = 0.1, \varepsilon = 0.1, t = 0.5$.

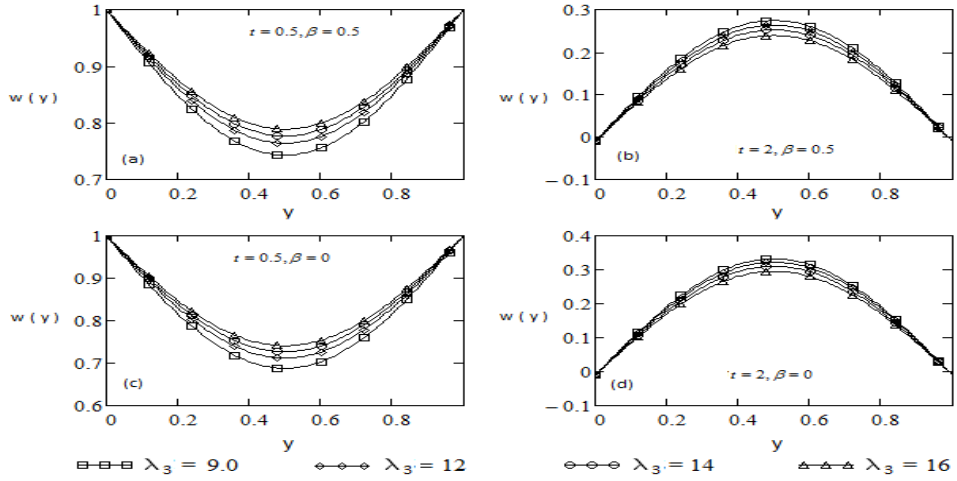

Fig. 2. Velocity profiles for duct motion induced by sawtooth pulses for Generalized Burgers' fluid for different values of λ_3. Other parameters and values are taken as $x = 0.5,\ \lambda_1 = 17,\ \lambda_2 = 4, \lambda_4 = 8,\ T = 1, \Omega = 0.1, \varepsilon = 0.1, t = 0.5$.

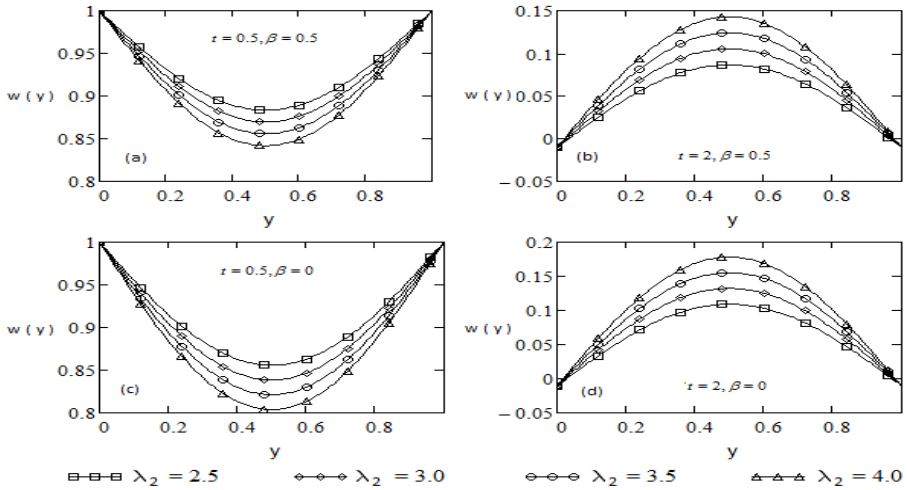

Fig. 3. Velocity profiles for duct motion induced by sawtooth pulses for Generalized Burgers' fluid for different values of λ_2. Other parameters and values are taken as $x = 0.5,\ \lambda_1 = 3,\ \lambda_3 = 2, \lambda_4 = 8,\ T = 1, \Omega = 0.1, \varepsilon = 0.1, t = 0.5$.

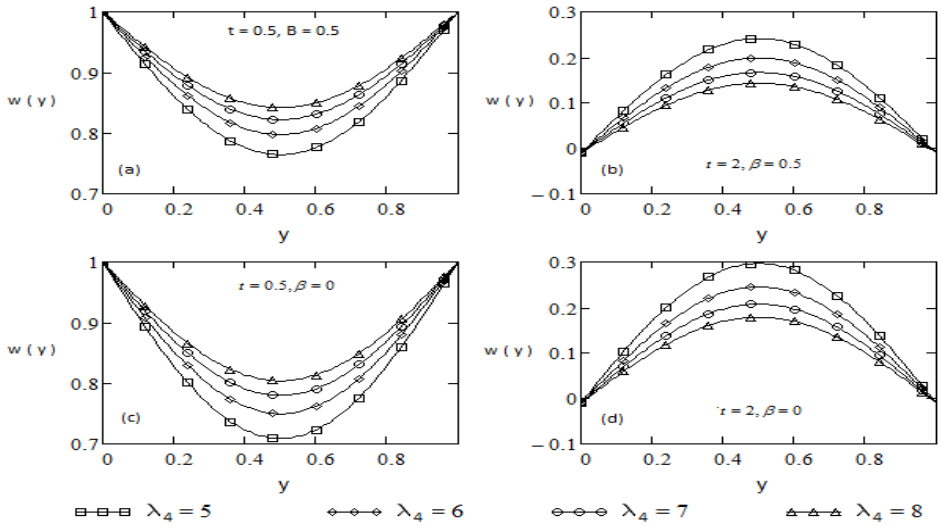

Fig. 4. Velocity profiles for duct motion induced by sawtooth pulses for Generalized Burgers' fluid for different values of λ_4. Other parameters and values are taken as $x = 0.5,\ \lambda_1 = 3,\ \lambda_2 = 4, \lambda_3 = 2, T = 1,\ \Omega = 0.1, \varepsilon = 0.1, t = 0.5$.

retarding flow corresponds to $t = 2$. Figs. (1a) and (1b) show that the magnitude of velocity profile is an increasing function of λ_1 for developing and retarding flows in the presence of side walls. Figs. (1c) and (1d) show that the effect of λ_1 on the velocity profile for both developing and retarding flow in the absence of side walls is same as in the presence of side walls. It is seen that the magnitude of velocity profile increases for both the developing and retarding flows. From these Figures it is also clear that the magnitude of velocity profile in the absence of side walls is greater than the magnitude of velocity profile in the presence of side walls. Fig. (2) displays the variations of the retardation time λ_3 from 9 to 16 on the velocity profile. It is seen that the magnitude of velocity profile decreases for both the developing and retarding flows in the presence as well as in the absence of side walls. Thus, both the parameters, λ_1 and λ_3 as expected, have opposite effects on the magnitude of velocity profile. Figs. (3) and (4) display the variations of the material parameters λ_2 and λ_4 on the velocity profile. It is seen that the magnitude of velocity profile is an increasing function with respect to λ_2 and a decreasing function with respect to λ_4 for all the four cases.

Figures 5, 6 and 7 are sketched in order to compare the various fluid types. Also, the influence of magnetic field, permeability and the period of saw-tooth pulses on the velocity fields is studied by means of numerical calculus and graphical illustrations. In these figures we have considered the following values of dimensionless coefficients: $\lambda_1 = 2.9,\ \lambda_2 = 4,\ \lambda_3 = 0.35,\ \lambda_4 = 3,$ $x = 0.4,$ and $y = 0.2$. Fig. 5 shows the diagrams of velocity $w(x,y,t)$, verses t, for the porosity parameter $\varepsilon = 0.5$, the pulses period T = 0.8 and for three values of the magnetic parameter $\Omega = 1.3, 2.8, 6$. In figure 5, we observe that there is a time- interval in which the velocity has an oscillating behavior for all kinds of fluids. After this moment, velocities tend to a common value (the differences between velocities of different fluids are insignificant). For low values of the magnetic field strength, amplitudes of the velocity oscillations are smaller for the generalized Burgers, Oldroyd-B and Newtonian fluids and much larger for Maxwell and Burgers fluids (see diagrams for $\Omega = 1.3$). If the magnetic field is stronger, the velocity amplitudes of Maxwell and Burgers fluids decrease while, the velocity amplitudes of generalized Burgers and Newtonian fluids increase (case $\Omega = 6$). It is important to note that, velocities of the fluids tend to a common value in shorter time if the magnetic field is stronger.

Figure 6 is plotted for fixed values of magnetic field strength and period of pulses, $\Omega = 2, T = 0.8$ and for three values of the porosity parameter $\varepsilon = 0.4, 0.75, 1$. In this case, amplitudes of the velocity oscillations of generalized Burgers, Oldroyd-B and Newtonian fluids are lower than those corresponding to the Burgers and Maxwell fluids. Increasing permeability leads to the increasing of the velocity amplitudes.

The effect of pulses period T on the velocity fields is shown in Figure 7. This figure is sketched for $\varepsilon = 0.5, \Omega = 2.5$, and three values of the parameter T, $T = 0.5, 1, 1.25$. The Burger fluid oscillates with larger amplitudes, while other fluids have oscillations with amplitudes close as order of magnitude. For low values of the parameter T, velocities tend to a common value in a shorter time than in the case of large values of the parameter T.

In order to study the influence of the magnetic parameter Ω and porous parameter $\mathcal{E}$ on the velocity field, we use a numerical procedure for the inverse Laplace transforms, namely the Stehfest's algorithm, Stehfest (1970). If we denote by $W(x,y,q)$ the inverse Fourier transform of the function given by Eq. (26), then, in accordance with Stehfest's algorithm, the inverse Laplace transform, namely the velocity field w(x,y,t) is given by

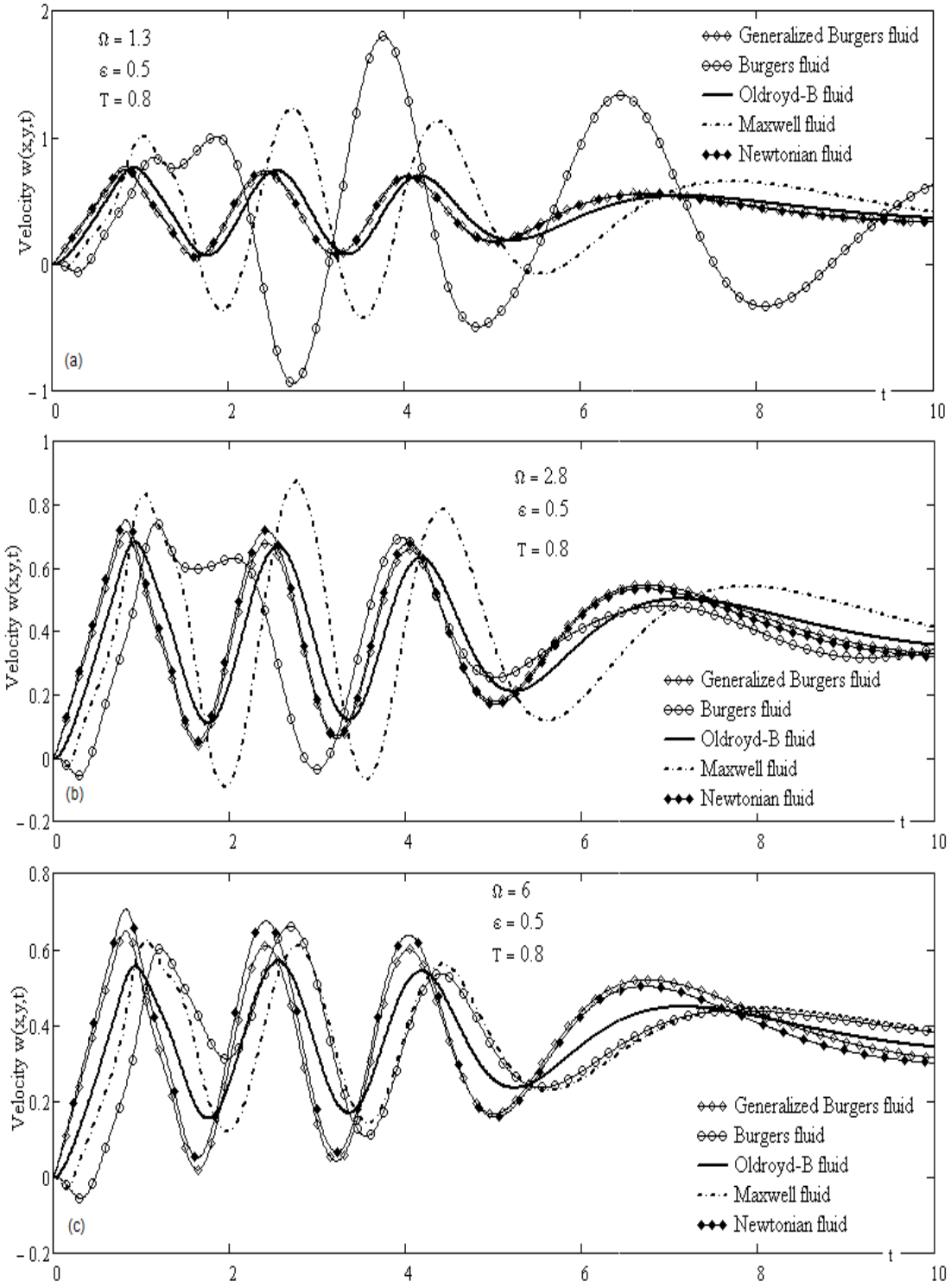

Fig. 5. Diagrams of the velocity w(x, y, t) for different values of magnetic parameter Ω. Comparison between five models for $\lambda_1 = 2.9$, $\lambda_2 = 4$, $\lambda_3 = 0.35$, $\lambda_4 = 3$, $x = 0.4$, and $y = 0.2$.

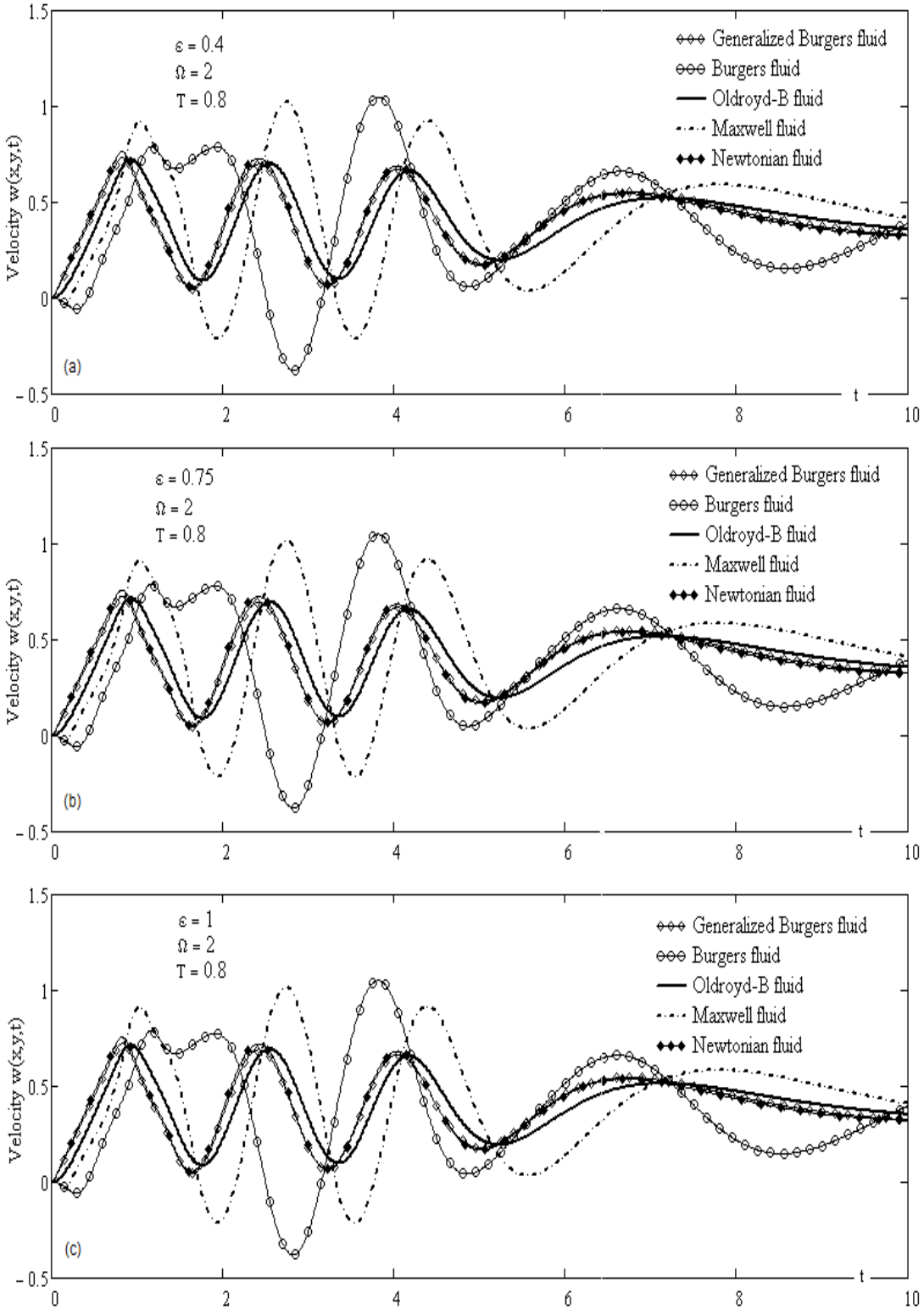

Fig. 6. Diagrams of the velocity w(x, y, t) for different values of the porosity parameter ε. Comparison between five models for $\lambda_1 = 2.9$, $\lambda_2 = 4$, $\lambda_3 = 0.35$, $\lambda_4 = 3$, $x = 0.4$, and $y = 0.2$.

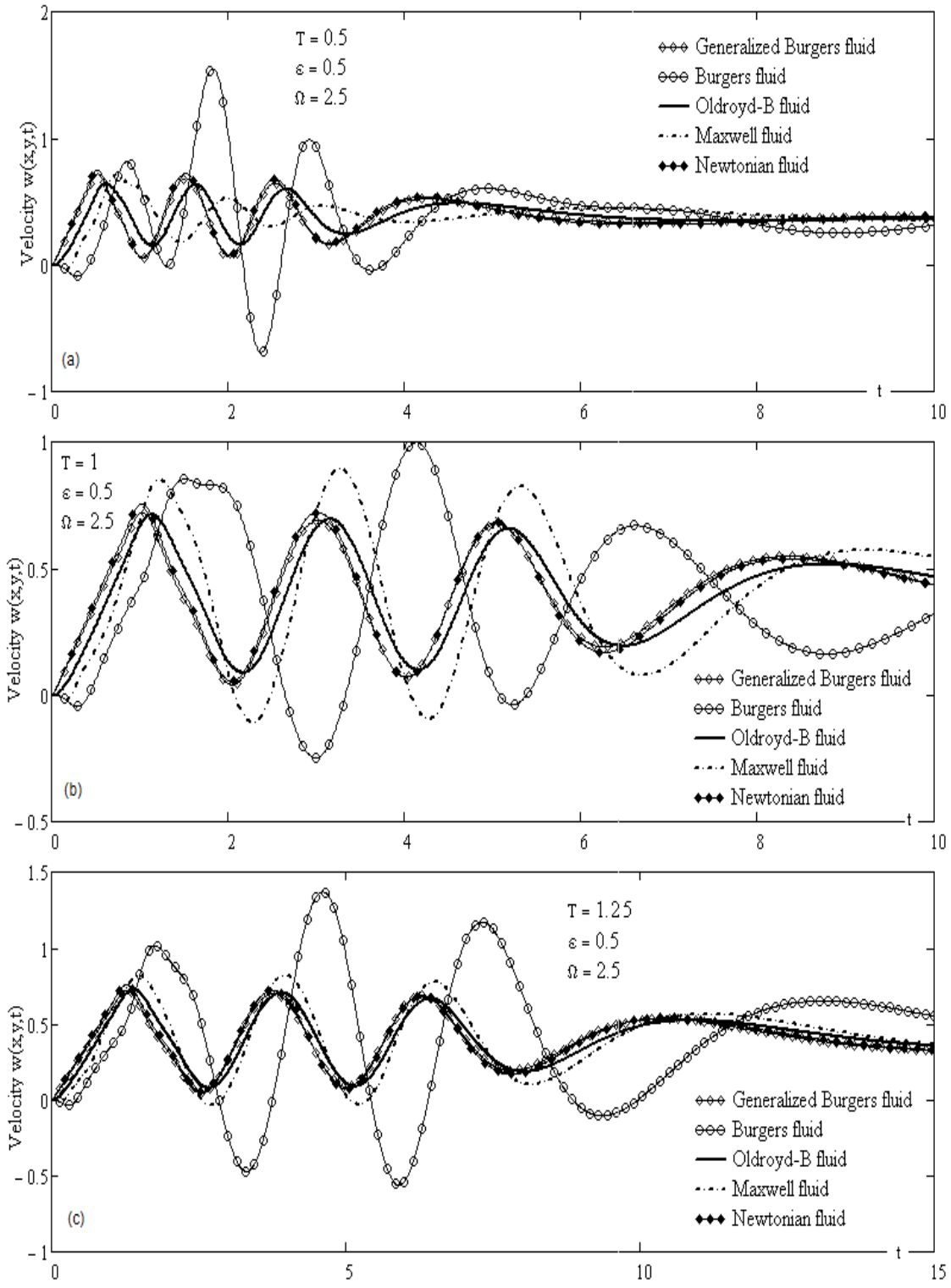

Fig. 7. Diagrams of the velocity $w(x, y, t)$ for different values of the parameter T. Comparison between five models for $\lambda_1 = 2.9$, $\lambda_2 = 4$, $\lambda_3 = 0.35$, $\lambda_4 = 3$, $x = 0.4$, and $y = 0.2$.

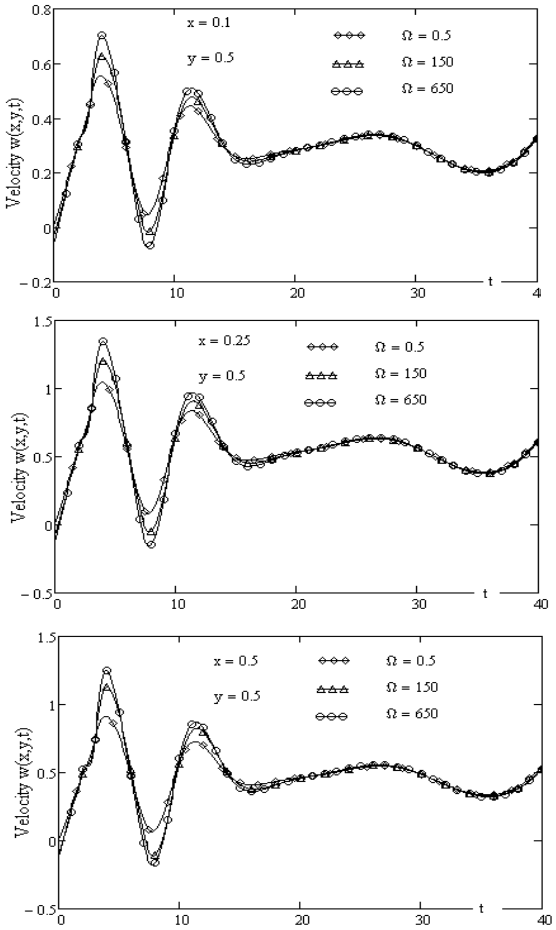

Fig. 8. The influence of magnetic parameter on the velocity field for T = 4, β =1.5, ε = 0.5, λ_1=2, λ_2= 0.7, λ_3=13, λ_4=3

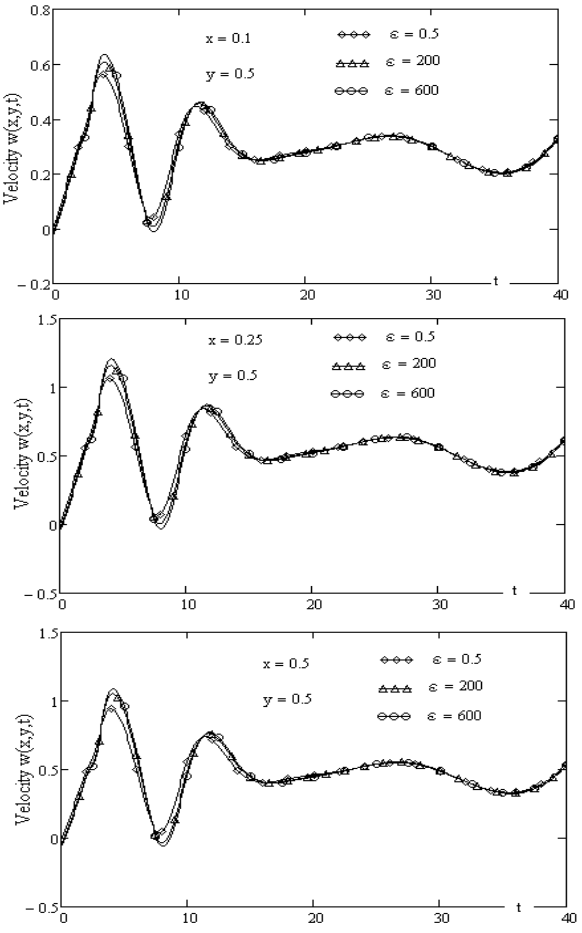

Fig. 9. The influence of porous parameter on the velocity field for T = 4, β =1.5, Ω = 10, λ_1=2, λ_2= 0.7, λ_3=13, λ_4=3

$$w(x,y,t)=\frac{\ln 2}{t}\sum_{j=1}^{2s} d_j\, W(x,y,j\frac{\ln 2}{t})$$

Where

$$d_j=(-1)^{j+s}$$
$$\sum_{i=\left[\frac{j+1}{2}\right]}^{\min(j,s)}\frac{i^s(2i)!}{(s-i)!i!(i-1)!(j-i)!(2i-j)!}$$

s is a positive integer number and $[r]$ denotes the integer part of the real number r. The influence of the magnetic parameter Ω on the velocity field is shown in Figure 8. From these diagrams, we observe that the influence of magnetic field is significant into a short interval of time after which, the differences between the velocities corresponding to different values of the magnetic parameter are insignificant. Also, be noted that for a strong magnetic field, the fluid flows faster. The velocity values increase from the wall to inside of the channel. Figure 9 is drawn to show the effect of porosity on the fluid velocity. Note that, after a certain moment of time, the influence of the porosity parameter on the fluid velocity is insignificant.

5. CONCLUSSIONS

Here we obtained analytical solutions for the magnetohydrodynamic flow of a generalized Burgers' fluid through a porous rectangular cross-section. The expressions for the velocity field and the corresponding tangential stresses induced by the velocity saw tooth pulses are obtained by means of the Laplace and double Fourier sine transforms in this order. The main findings are summarized as follows:

- The magnitude of velocity profile is an increasing function with respect to λ_1, λ_2 and a decreasing function with respect to λ_3, λ_4 for both developing and retarding flows in the absence as well as in the presence of side walls.
- The magnitude of velocity profile is greater in the absence of side walls as compared to that in the presence of side walls.
- Magnitudes of velocity profiles tend to a common value in shorter time as the magnetic field becomes stronger.
- Increasing permeability leads to increase the velocity amplitudes.
- For low values of the time period T, velocities

tend to a common value in a shorter time as compared to large values of the parameter T .

- For a much strong magnetic field, the fluid flows faster.

ACKNOWLEDGMENT

The authors are thankful to the honorable reviewers for their fruitful suggestions for improvement of the paper.

REFERENCES

Fetecau, C., A.U. Awan and Cor. Fetecau (2009). Taylor-Couette flow of an Oldroyd-B fluid in a circular cylinder subject to a time-dependent rotation. *Bull. Math. Soc. Sci. Math. Roumanie*, 52, 117-128.

Fetecau, C. and Cor. Fetecau (2005). Unsteady flows of Oldroyd-B fluids in a channel of rectangular cross-section. *International Journal of Non-Linear Mechanics*, 40, 1214-1219.

Ghosh, A.K. and P. Sana (2008). On hydromagnetic channel flow of an Oldroyd-B fluid induced by tooth pulses. *Magnetohydrodynamics*, 44, 325-340.

Hunt, J.C.R. (1965) Magnetohydrodynamic flow in rectangular ducts, *Journal of Fluid Mechanics*, 21, 577-590.

Jarrahi, M., C. Castelain and H. Peerhossaini (2011). Laminar sinusoidal and pulsatile flows in a curved pipe. *Journal of applied fluid mechanics* 4(2), 21-26.

Johri, A.K. and M. Singh, (1998). Oscillating flow of a viscous liquid in a porous rectangular duct. *Def. Science Journal*, 38, 21-24.

Khan, M. and A. Anjum, (2012). Some oscillating motions of a Burgers' fluid. *International Journal of Physical Sciences*, 4, 5834-5851.

Khan, M., C. Fetecau and T. Hayat, (2007). MHD transient flows in a channel of rectangular cross-section with porous medium. *Physics Letters A*, 369, 44-54.

Khan, M. and Zeeshan, (2011). MHD flow of an Oldroyd-B fluid through a porous space induced by sawtooth pulses. *Chinnese Physics Letters*, 28, 84701-84704.

Nazar, M., F. Shahid, F.S. Akram, and Q. Sultan, (2012). Flow on oscillating rectangular duct for Maxwell fluid, *Applied Mathematics and Mechanics Engl. Ed*., 33, 717-730.

Mahmood, A., C. Fetecau, N.A. Khan, N.A. and M. Jamil, (2010). Some exact solutions of the oscillatory motion of a generalized second grade fluid in an annular region of two cylinders. *Acta Mechanica Sinica*, 26, 541-550.

Seth, G.S., Md. S. Ansari and R. Nandkeolyar (2011). Effects of rotation and magnetic field on unsteady coquette flow in a porous channel. *Journal of applied fluid mechanics*, 4(2), 95-103.

Seth, G.S. and J.K. Singh (2013). Effects of hall current on unsteady MHD couette flow of class-II in a rotating system. *Journal of applied fluid mechanics*, *6(*4), 473-484.

Sultan, Q., M. Nazar, W. Akhtar and U. Ali, (2013a). Unsteady flow of a Maxwell fluid in a porous rectangular duct. *Science International*, 25, 181-194.

Sultan, Q., M. Nazar, U. Ali and M. Imran, (2013b). Unsteady flow of oldroyd-b fluid through porous rectangular duct. *International Journal of Nonlinear Science*, 15, 195-211.

Stehfest, H. (1970), Algorithm 368: Numerical inversion of Laplace transform, *Communication of the ACM* 13 (1), 47-49.

Tsangaris, S. and N. W. Vlachakis, (2003). Exact solution of the Navier-Stokes equations for the oscillating flow in a duct of a cross-section of right-angled isosceles triangle. *Z. angew. Math. Physics*, 54, 1094-1100.